ELSEVIER

Polymer 42 (2001) 963–969

polymer

www.elsevier.nl/locate/polymer

Interactions between wood polymers studied by dynamic FT-IR spectroscopy

M. Åkerholm, L. Salmén*

Swedish Pulp and Paper Research Institute (STFI), Box 5604, S-11486 Stockholm, Sweden

Received 17 February 2000; received in revised form 26 May 2000; accepted 12 June 2000

Abstract

Dynamic FT-IR spectroscopy was applied to study the mechanical interactions among cellulose, xylan and glucomannan in spruce wood fibers. The understanding of these interactions is of importance in controlling the physical properties of the fibers in different processes. A multivariate analysis demonstrated that the different carbohydrate polymers could be spectrally separated. These specific wavenumbers were then used to study the response of the wood polymers to a small sinusoidal tensile strain. The results showed a difference in mechanical behavior of the polymers depending on the loading direction toward the fiber axis. In parallel loading the results suggested a close cooperation between cellulose and glucomannan in the fiber wall, whereas xylan showed no mechanical interaction with cellulose.
© 2000 Elsevier Science Ltd. All rights reserved.

Keywords: Dynamic FT-IR spectroscopy; Wood polymers; Mechanical interactions

1. Introduction

The physical and mechanical properties of wood fibers are of great importance for their use in different paper grades. These fiber properties are mainly determined by the arrangement of the polymers within the cell wall: the cellulose, the hemicelluloses (xylan and glucomannan) and the lignin, and the interactions among them. This arrangement is still not fully understood and many models have been suggested for the structural organization of the wood polymers in the fiber wall. The first models treated the cell wall as more or less a composite of almost separate layers [1,2]. More recent studies of the biogenesis of wood cell walls indicate a much more intimate mixing of the components [3]. To better understand the roles of the hemicelluloses and the lignin in the wood cell wall, several studies have been performed on bacterial cellulose production in the presence of wood hemicelluloses or lignin–carbohydrate complexes (LCCs) [4–7]. Atalla et al. [4] suggested from such a study that the hemicelluloses act as regulators for the cellulose aggregation and that they are well integrated into the cellulose structure. In a study with LCCs [7] it was found that lignin did not influence the cellulose aggregation but it was suggested as essential for the formation of a firm cellulose–hemicellulose–lignin framework in the secondary cell wall. The same study concluded that glucomannan polysaccharides had higher affinity to cellulose than xylan polysaccharides, whereas other studies suggest the opposite [5]. Common conclusions are still that the different types of hemicelluloses have different effects on the structure of bacterial cellulose and therefore probably also play different roles in the wood fiber cell wall. In extraction procedures of wood, the glucomannan is more difficult to separate from cellulose than xylan. From this, some aggregation of the glucomannan on the surface of the cellulose microfibrils has been assumed [8].

In order to improve the fiber processing, it is important to identify how the different wood polymers affect the mechanical properties of the fiber [9]. The extent to which a polymer contributes to the mechanical properties of a composite is dependent both on the directional arrangement and on the domain size of the individual polymer [10]. Since lignin macromolecules extracted from pulp fibers have been reported to have a larger diameter [11,12] than the domain size required to affect the properties [13], the individual properties of lignin are expected to show up in the fiber properties. Indeed, a glass transition temperature characteristic of the lignin component has been identified from measurements on wood [14,15]. The role of the hemicelluloses in the mechanical sense is more questionable. Are the

* Corresponding author. Tel./fax: +46-8-411-55-18.
E-mail addresses: margaretha.akerholm@stfi.se (M. Åkerholm), lennart.salmen@stfi.se (L. Salmén).

0032-3861/01/$ - see front matter © 2000 Elsevier Science Ltd. All rights reserved.
PII: S0032-3861(00)00434-1

Table 1
Composition of holocellulose fiber samples

Sample number	Lignin (%)	Xylan (%)	Glucomannan (%)	Cellulose (%)
1	3	11	22	64
2	1	8	16	75
3	<1	7	17	76
4	<1	5	16	78
5	<1	2	16	82
6	<1	2	9	89
7	<1	1	6	92
8	1	5	22	72
9	1	4	17	78
10	1	5	20	74
11	<1	2	5	92
12	<1	1	5	93
13	1	2	12	85

hemicelluloses too closely integrated with the other cell wall components to be able to act as separate polymers? A close mixing of the wood polymers has been indicated by differences in the softening behavior of wood as shown by the selective removal of the different wood polymers in studies with Dynamic Mechanical Analysis (DMA) [16]. Based on these measurements the authors suggested a new cell wall model where the xylan is associated with the lignin and the glucomannan is associated with the cellulose.

DMA is a useful tool for characterizing the mechanical properties of polymeric materials. However, it gives no information of these characteristics on the molecular level. FT-IR spectroscopy, on the other hand, gives molecular information but no information about the mechanical properties. In a newly developed technique, dynamic FT-IR spectroscopy (or DMA-FTIR) [17], these two characterization techniques are combined to study the mechanical interactions between and within polymers on the molecular level. The first study on cellulosic material with this technique demonstrated the separation of the broad OH-range absorption band into several distinct bands for the inter- and intramolecular hydrogen bonds [18]. The present study has applied dynamic FT-IR spectroscopy to study how the wood polymers interact in the wood fiber wall.

2. Experimental

2.1. Materials

Holocellulose was prepared from chips of Norway spruce (*Picea Abies*) by acetone extraction to remove extractives followed by sodium chlorite extraction in acetate buffer to remove lignin. Two different holocelluloses were made, one extracted for 96 h at 50°C and one extracted for 79 h at 70°C. From these holocellulose pulps, samples with different amounts of hemicellulose were prepared by alkaline extraction in a nitrogen atmosphere. The alkali concentration varied between 1 and 25% (KOH or NaOH) with addition of boric acid (0–8%) [19]. The extractions were carried out at room temperature. Sugar analyses were made on all fiber samples and the polymer compositions were calculated according to Janson [20], see Table 1. All 13 samples were used for a multivariate study of static spectra, while only sample number 1 (11% xylan, 22% glucomannan, 64% cellulose and 3% lignin) was studied by dynamic FT-IR measurements.

2.1.1. Sheets

Thin sheets (20 g/m^2) were made from all fiber samples on a Formette Dynamique at a speed of rotation of 1400 rpm, which gave well-orientated sheets. Before sheet formation, all samples were homogenized by pumping the pulp several times through a slit of 0.3–0.4 mm in a laboratory homogenizer (Gaulin Corp.).

2.2. Methods

2.2.1. Static FT-IR measurements

All spectra were recorded on a Bio-Rad FTS 6000 FT-IR spectrometer. Transmission spectra were recorded with a resolution of 8 cm^{-1} for each fiber sample (as sheet) in rapid scan mode using a liquid nitrogen cooled MCT (Mercury Cadmium Telluride) detector. The spectra were converted to the absorbance mode and baseline corrected at 10 points. The intensities between 3950 and 700 cm^{-1} of each spectrum were used as variables in the multivariate data analysis.

2.2.2. Multivariate data analysis

In order to find specific wavenumbers for each of the carbohydrate polymers in the used spruce holocellulose pulps a multivariate model was calculated for each polymer using Partial Least-Squares (PLS) regression [21]. The static spectra were used as *x*-variables and the polymer composition was used as the *y*-variable. There were 13 objects in each model, where both *x*-variables and the *y*-variable were mean-centered. All calculations were performed using the EXTRACT 3.0 software [22].

2.2.3. Dynamic FT-IR measurements

In polymer research, dynamic IR spectroscopy combined with two-dimensional (2D) correlation analysis [23] has been used for several years. This technique is a powerful tool for studying the time-dependent response of a sample as a function of an applied perturbation. Furthermore, by applying the 2D correlation analysis it is possible to identify intra- and intermolecular interactions in polymers. Also, the ability to resolve overlapping spectral bands is enhanced because they are spread out over the second spectral dimension. The first studies using dynamic IR spectroscopy were performed on dispersive IR and rapid scanning FT-IR instruments, but in 1991 Palmer et al. [24] introduced the use of step-scan interferometry to dynamic FT-IR

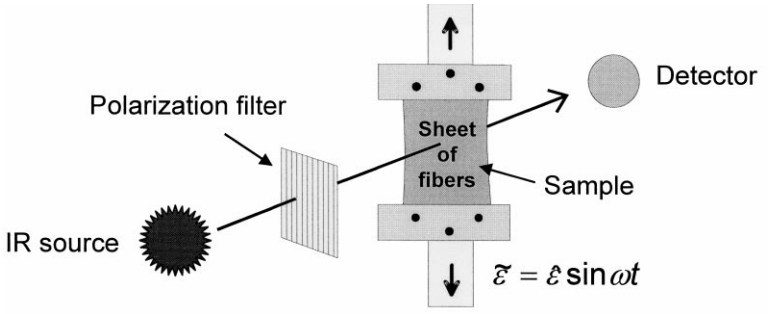

Fig. 1. Schematic description of dynamic FT-IR spectroscopy with sinusoidal strain as perturbation method. The strain variation $\tilde{\varepsilon}(t)$ is equal to the strain amplitude $\hat{\varepsilon}$ times its variation with time sin ωt where ω is the frequency and t the time.

spectroscopy. The step-scan technique decouples the spectrum from the time domain, allowing the time-dependent response of the sample to be retrieved more conveniently. In Fig. 1 a schematic description of the experimental set-up can be seen.

Oriented sheets of holocellulose (sample number 1) were studied. Samples with the dimension 22×30 mm^2 were cut out and tightened by applying a preload of about 30% of the stress at break of the sample in the Polymer Modulator [25]. Before starting a measurement, the samples were dried inside the purged sample compartment for 1 h. A small amplitude sinusoidal strain ($<0.3\%$) with a frequency of 16 Hz (chosen as the most suitable within the frequency range of the instrument, 5–50 Hz) was applied to the sample while the FT-IR spectra were being collected. The interferometer was run in step-scan mode and the same detector and resolution were used as for static spectra. Four scans were co-added in each measurement and the required measurement time was about 2.5 h. The incident IR radiation was polarized at either 0 or 90° in relation to the stretching direction. The holocellulose sheets were loaded in two different modes, parallel or perpendicular to the main fiber direction. The strain amplitude was equal for both loading modes, but for the perpendicular stretched sample the preload was higher in relation to its stress at break (about 60%). All the dynamic spectra were normalized by division with the static transmission spectrum, baseline corrected and smoothed.

With the perturbation of the sample the molecules within it are affected in different ways depending on their local molecular environment. The electrical dipole-transition moments, giving absorption bands in a static spectrum, could either be unaffected, change in direction or change in conformation. A dynamic spectrum shows only changes in spectral intensity as a result of the perturbation. In other words, there will be no absorption bands for the unaffected groups in such spectra. Since the incident IR radiation is polarized, there will also be a change in absorption intensity if the molecular vibration changes in direction, resulting in a positive or negative absorption band in the dynamic spectrum. If a chemical bond is affected in such a way that its vibrational energy is changed there will be a so-called split absorption band in the dynamic spectrum, one positive and one negative band directly connected to each other. To be able to study time-dependent movements of the molecular groups, the dynamic spectrum is divided into two orthogonal parts. The in-phase spectrum represents the elastic component of the sample and is the direct response of molecular groups, while the out-of-phase spectrum represents the viscous component of the sample and derives from time-delayed responses.

2.2.4. Correlation analysis

By applying a simple correlation analysis (Appendix A), the dynamic FT-IR spectra can be transformed into a pair of the so-called 2D FT-IR correlation spectra, referred to as the synchronous and the asynchronous 2D spectrum, respectively. These correlation spectra are in fact three-dimensional with independent wavenumbers on the x- and y-axis, and correlation intensities on the z-axis. The synchronous spectrum is symmetric with respect to the diagonal line and the correlation intensities display similarities in time-dependent movements. Since every vibration is correlated with itself, there are peaks on the diagonal (autopeaks) for every molecular vibration affected by the applied strain. If the intensity at two different wavenumbers fluctuates with the same time-dependent behavior, there will be an off-diagonal peak (crosspeak) in the spectrum, indicating that these two groups are affected in the same way by the applied perturbation. This information is then used to draw conclusions about interactions between polymers.

In the asynchronous spectrum only independent fluctuations of the IR signals are displayed. There are no peaks on the diagonal in this spectrum, or will there be any off-diagonal peaks for a totally elastic sample, because there are no time-delayed movements. For a viscoelastic sample the asynchronous spectrum is useful to achieve resolution of overlapping bands.

3. Results and discussion

3.1. Multivariate study

The static spectra of 13 sheets of different polymer

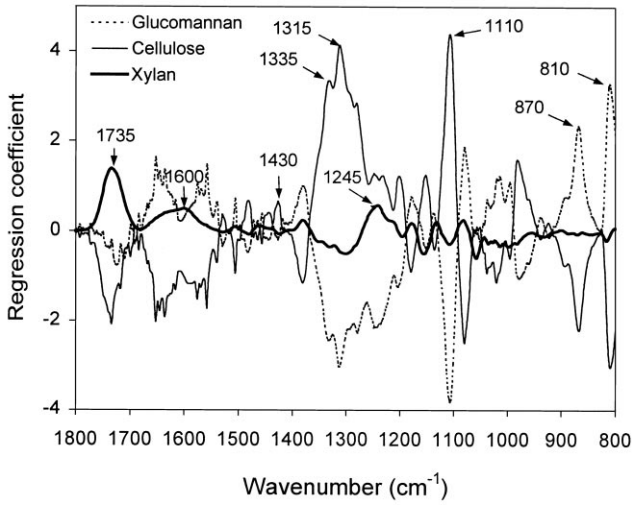

Fig. 2. Regression coefficients from PLS-models for each of the carbohydrate polymers in wood.

composition were used to make the multivariate analysis. The regression coefficients of the wavenumbers between 1800 and 800 cm^{-1} from PLS-models of each carbohydrate polymer are given in Fig. 2. Since these coefficients represent the correlation for each wavenumber to the polymer concentration (*y*-variable), these graphs were used to find specific wavenumbers that could separate the polymers when evaluating the dynamic spectra. For cellulose and glucomannan the models were based on four principal components (pcs), while the model for xylan was based only on three pcs. The bands at 1735, 1600 and 1245 cm^{-1} showed strongest correlation to the concentration of xylan. This is in agreement with the literature, where these bands are assigned to different vibrations from the carboxylic acid (and carboxylate ion) group in the 4-*O*-methyl-D-glucuronic acid substituents in the xylan [26,27]. The strongest correlation to the glucomannan concentration was seen at 810 and 870 cm^{-1}. These bands are, respectively, assigned to the in-phase ring stretching and to the deformation of the equatorial C2–H bond of the mannose residue [26,28,29]. For cellulose there are no specific chemical groups differing from the other polymers, although there were strong correlations between the cellulose concentration and some bands around 1300 cm^{-1}. This region is strongly affected by the crystallinity of the polysaccharide and since cellulose is more crystalline than the hemicelluloses, cellulose has sharper and more intense absorption bands in this region [30]. Therefore, the bands at 1315 (CH_2 wagging) and 1335 cm^{-1} (O–H in-plane bending) were used as specific for the crystalline cellulose polymer. The cellulose PLS-model also showed some correlation to the band at 1430 cm^{-1} (CH_2 scissoring), which is often used for crystallinity indexes [30]. The very strong correlation to the band at 1110 cm^{-1} is also a result of the crystallinity [31], although this band is not used for cellulose in this study due to the generally high absorption in this region. The differences in IR absorption between cellulose and the glucose containing hemicellulose in the 1300–1450 cm^{-1} region were verified by recording spectra of spruce cellulose and extracted spruce glucomannan with DR (Diffuse Reflectance)-FTIR spectroscopy (Fig. 3). Absorption bands at 1315, 1335 and 1430 cm^{-1} are well resolved in the cellulose spectrum while these are less distinct or absent in the glucomannan spectrum.

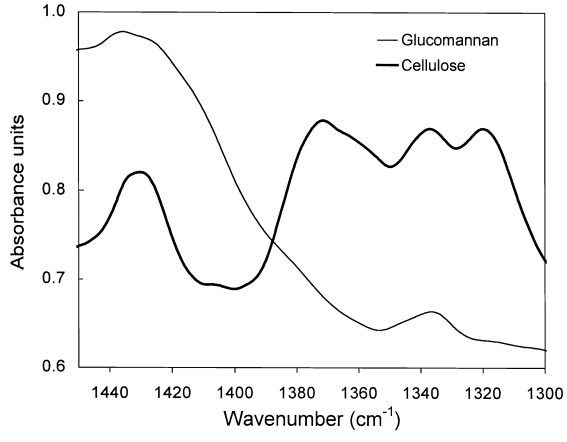

Fig. 3. DR-FTIR spectra of spruce cellulose and extracted spruce glucomannan.

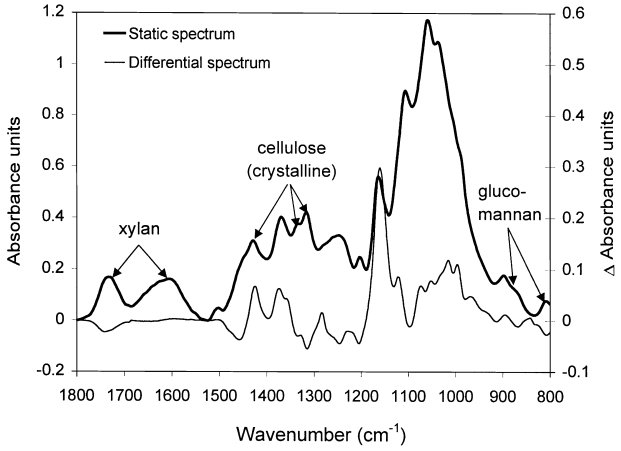

Fig. 4. Static and differential (0–90° polarization) spectrum of the holocellulose sample used for dynamic measurements.

3.2. Polymer orientation

In the interpretation of the dynamic spectra, the abovementioned specific wavenumbers were used for the different polymers as indicated in the static spectrum of the holocellulose sheet studied (Fig. 4). In Fig. 4 a differential spectrum (0–90° IR polarization in relation to fiber direction) is also included. Positive peaks (vibration oriented parallel to the fiber axis) were seen for some of the specific cellulose bands (1110, 1430 cm^{-1}) while negative peaks were obtained for other (1315, 1335 cm^{-1}). The direction of these vibrations

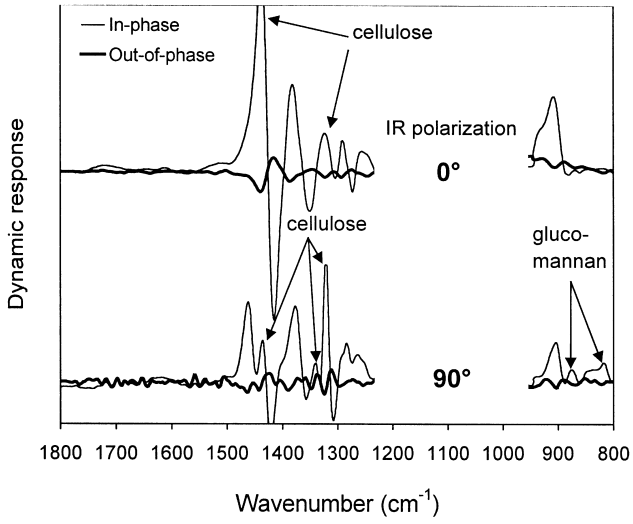

Fig. 5. Dynamic spectra of the holocellulose sample stretched parallel to fiber direction. The region between 1220 and 950 cm^{-1} has been omitted. The IR polarization is either parallel (0°) or perpendicular (90°) to the applied straining direction.

in relation to the cellulose backbone confirms a net orientation of the cellulose along the fiber axis. The strong positive peak at 1160 cm^{-1} originates from the antisymmetric bridge COC stretching mode [32]. This stretching mode is parallel to the chain axis and is often used as a measure of the orientation of cellulose polymers. As all of the carbohydrates examined are connected by COC bridges, it can in this case not be used to determine the direction of any specific polymer. Both of the glucomannan bands (810, 870 cm^{-1}) gave negative peaks in the differential spectrum. As these vibrations are oriented almost orthogonal to the glucomannan backbone, these data are consistent with earlier suggestions of an orientation of the glucomannan in parallel to the cellulose microfibrils [27,33]. For the xylan only a weak negative peak was observed at 1735 cm^{-1} suggesting a more or less isotropic arrangement.

3.3. Dynamic FT-IR measurements

The dynamic spectra, in-phase and out-of-phase, of the holocellulose sample stretched parallel to fiber direction are shown in Fig. 5 for the region 1800–800 cm^{-1}. The upper two spectra are the result with 0° polarization of the incident IR radiation (the same direction as that of the stretching) and the lower two are recorded with 90° polarization. Since the various C–O vibrations, with absorbance between 1220 and 950 cm^{-1}, dominate the spectra and since these are not discussed in this study, this spectral region has been omitted from the figure. The weak intensity of the out-of-phase spectra indicated a more or less elastic response of the wood polymers to the dynamic strain, which means that there were no molecular groups with a time-delayed response. The strong carbonyl bands of xylan from the static spectrum (Fig. 4) could not be found in any of the dynamic spectra with a loading parallel to the fibers. This means that xylan was unaffected by the applied strain. From cellulose there were clear dynamic peaks for both polarization directions, which is a consequence of this polymer taking most of the load in the fiber when deformed. The behavior of glucomannan differs between the polarization directions. Although the specific bands of the polymer at 810 and 870 cm^{-1} were very weak in the static spectra, they could be seen in the 90° dynamic in-phase spectrum, but not in the 0° spectrum. The glucomannan moves in the structure because of the applied strain, but only the IR response of the polymer chains oriented parallel to the deformed cellulose is affected. Because of the orthogonal vibrational response to the chain axis of the glucomannan, a peak in 90° polarization means that the polymer chains affected are oriented parallel to the strain direction, which in this case is also the fiber direction and the main direction of the cellulose microfibrils.

3.4. Two-dimensional correlations

To study the interactions between cellulose and

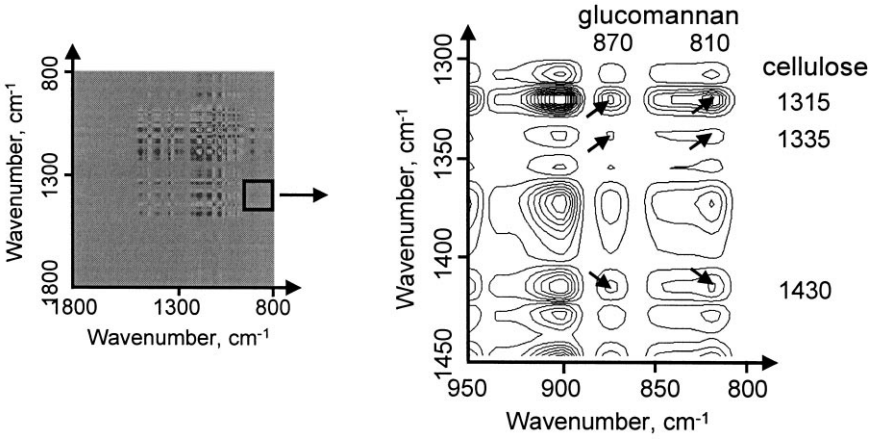

Fig. 6. Synchronous 2D spectrum of the holocellulose sample stretched parallel to fiber direction by 90° polarization of the IR beam. To the left the whole region is shown, to the right there is an enhancement of the off-diagonal area marked in the left figure.

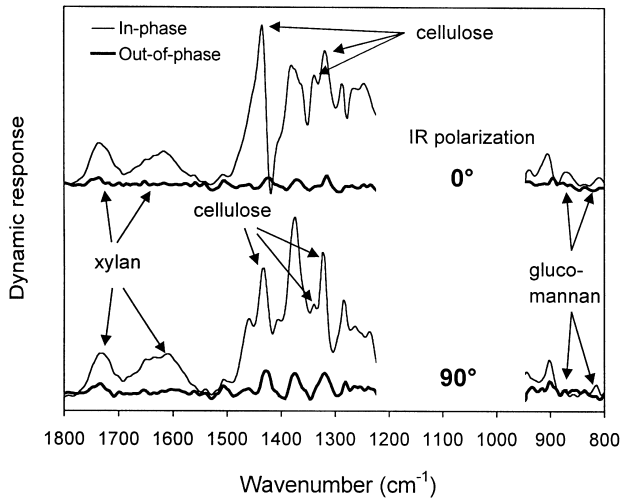

Fig. 7. Dynamic spectra of the holocellulose sample stretched perpendicular to fiber direction. The region between 1220 and 950 cm^{-1} has been omitted. The IR polarization is either parallel (0°) or perpendicular (90°) to the applied straining direction.

glucomannan, cross peaks in a 2D FT-IR spectrum were examined. Fig. 6 (left) gives the synchronous 2D spectrum of the chosen region for the parallel stretched sample in 90° polarization. On the diagonal there are peaks from all affected absorption bands. As in the present study the out-of-phase response is negligible compared to the in-phase response: all the diagonal peaks will show off-diagonal correlation intensities (cross peaks), representing similar time-dependent movements of the different molecular groups. To the right in Fig. 6, an enhancement of the 2D spectrum is shown. This is an off-diagonal part of the spectrum displaying only cross peaks with the specific bands of cellulose on the *y*-axis and the specific bands of glucomannan on the *x*-axis. The appearance of cross peaks between all specific bands of cellulose and those of glucomannan reveals that the two polymers moved synchronously as a consequence of the applied dynamic strain, a fact that can be seen already from the dynamic spectra (Fig. 5). This implies strong interactions between the two polymers and together with the analysis of the differential spectrum this confirms the idea of glucomannan being oriented parallel to the cellulose.

3.5. Effect of orientation

The dynamic spectrum for a loading perpendicular to the main fiber direction looked quite different (Fig. 7). Besides the cellulose response, there were dynamic peaks from both xylan and glucomannan in both polarization directions. In this case there were glucomannan and xylan chains affected by the applied strain oriented both parallel and perpendicular to the strain direction.

The difference in dynamic behavior of the hemicelluloses for different loading modes suggests that there are different interaction mechanisms operating in the different stretching experiments. When the sample is stretched parallel to the fiber direction most of the microfibrils are oriented in this direction, allowing them to take up the applied load. The stiffness of the microfibrils is reflected in the more or less total elastic response of the sample in this mode. The response of the glucomannan by 90° polarization, reflecting molecules oriented in parallel with the microfibrils, suggests a close cooperation between cellulose and glucomannan inside the fiber wall. From the observation of the different dynamic behavior of the xylan and the glucomannan it is clear that the two hemicelluloses are organized differently in the wood fiber wall. The results obtained in this study are in good agreement with the cell wall model suggested by Salmén and Olsson [16]. The glucomannan moves synchronously with the cellulose because of its strong association with the microfibrils, while the mechanical interaction of xylan with cellulose is more indirect.

In the other loading mode studied, perpendicular to the fiber orientation, the load-taking microfibrils are not oriented in the straining direction. Probably a deformation of cross fiber elements is occurring and thus the result should reflect more the interactions between polymers in the bonds between fibers or interactions across the fiber wall. The argument for this hypothesis is the absence of polarization differences (no direction of the hemicelluloses). In this case both of the hemicelluloses seem to be important for the interactions. If more evidence for the hypothesis can be found, this could be a new tool to study the effect of resorbed xylan in the pulping processes.

4. Conclusions

This study demonstrates that dynamic FT-IR spectroscopy is a useful tool for studying polymer dynamics in the wood fiber wall. It has also been shown that the cellulose and the hemicelluloses can be spectrally separated, which is necessary for the interpretation of dynamic spectra.

The measurements parallel to fiber direction have revealed a difference in mechanical behavior between the two main hemicelluloses in spruce wood, where the glucomannan has a closer association to cellulose than the xylan. This indicates different purposes for the two hemicelluloses in the wood fiber.

Acknowledgements

This work was carried out within the framework of Wood and Wood Fibre, a post-graduate school sponsored by the Swedish Council for Forestry and Agricultural Research and the Swedish University of Agricultural Sciences.

Appendix A

For a pair of time-dependent variations of IR signals

measured at two different wavenumbers, $\tilde{A}(\nu_1, t)$ and $\tilde{A}(\nu_2, t)$, the dynamic IR cross-correlation function $X(\tau)$ is defined as [23]

$$X(\tau) = \lim_{T\to\infty} \frac{1}{T} \int_{-T/2}^{T/2} \tilde{A}(\nu_1, t)\tilde{A}(\nu_2, t + \tau)\, \mathrm{d}t \tag{A1}$$

where τ is the correlation time. For an external sinusoidal perturbation with a fixed frequency ω

$$\tilde{\varepsilon}(t) = \hat{\varepsilon} \sin \omega t \tag{A2}$$

the IR intensity may be expressed as

$$\tilde{A}(\nu, t) = A'(\nu) \sin \omega t + A''(\nu) \cos \omega t \tag{A3}$$

where $A'(\nu)$ and $A''(\nu)$ are the orthogonal components, in-phase and out-of-phase, of the dynamic spectrum. Substituting Eq. (A3) into Eq. (A1), the IR cross-correlation function reduces to

$$X(\tau) = \Phi(\nu_1, \nu_2) \cos \omega t + \Psi(\nu_1, \nu_2) \sin \omega t \tag{A4}$$

where the synchronous and the asynchronous correlation intensities, $\Phi(\nu_1, \nu_2)$ and, $\Psi(\nu_1, \nu_2)$, of the dynamic spectrum, are given by

$$\Phi(\nu_1, \nu_2) = \frac{1}{2}[A'(\nu_1)A'(\nu_2) + A''(\nu_1)A''(\nu_2)], \tag{A5}$$

$$\Psi(\nu_1, \nu_2) = \frac{1}{2}[A''(\nu_1)A'(\nu_2) - A'(\nu_1)A''(\nu_2)]. \tag{A6}$$

References

[1] Fengel D. Tappi 1970;53(3):497–503.
[2] Kerr AJ, Goring DAI. Cellul Chem Technol 1975;9(6):563–73.
[3] Terashima N, Fukushima K, He L-F, Takabe K. Comprehensive model of the ligninfied plant cell wall. In: Jung HG, Buxton DR, Hatfield RD, Ralph J, editors. Forage cell wall structure and digestibility. Madison, WI: ASA-CSSA-SSSA, 1993. p. 247–70.
[4] Atalla RH, Hackney JM, Uhlin I, Thompson NS. Int J Biol Macromol 1993;15:109–12.
[5] Uhlin KI, Atalla RH, Thompson NS. Cellulose 1995;2(2):129–44.
[6] Tokoh C, Takabe K, Fujita M, Saiki H. Cellulose 1998;5(4):249–61.
[7] Iwata T, Indrarti L, Azuma J-I. Cellulose 1998;5(3):215–28.
[8] Fengel D. J Polym Sci: Part C 1971;9(36):383–92.
[9] Salmén L, Ljunggren S. Physicochemical aspects of fibre processing. In: Kennedy JF, Philips GO, Williams PA, editors. The chemistry and processing of wood and plants fibrous materials. Cambridge: Woodhead Publishing, 1996. p. 173–81.
[10] Kaplan DS. J Appl Polym Sci 1976;20:2615–29.
[11] Willis JM, Yean WQ, Goring DAI. J Wood Chem Technol 1987;7(2):259–68.
[12] Favis BD, Yean WQ, Goring DAI. J Wood Chem Technol 1984;4(3):313–20.
[13] Schick C, Donth E. Phys Scr 1991;43:423–9.
[14] Irvine GM. Tappi J 1984;67(5):118–21.
[15] Östberg G, Salmén L, Terlecki J. Holzforschung 1990;44(3):223–5.
[16] Salmén L, Olsson A-M. J Pulp Pap Sci 1998;24(3):99–103.
[17] Noda I, Dowrey AE, Marcott C. J Polym Sci, Polym Lett Ed 1983;21:99–103.
[18] Hinterstoisser B, Salmén L. Cellulose 1999;6(3):251–63.
[19] Nelson R. Tappi 1960;43(4):313–7.
[20] Janson J. Paperi Puu 1970;52(5):323–9.
[21] Geladi P, Kowalski B. Anal Chim Acta 1986;185:1–17.
[22] Lindeberg O. Norrköping, Sweden: Extract Information AB, 1999.
[23] Noda I. Appl Spectrosc 1990;44(4):550–61.
[24] Palmer RA, Manning CJ, Chao JL, Noda I, Dowrey AE, Marcott C. Appl Spectrosc 1991;45(1):12–17.
[25] Manning C, Troy ID. Manning Applied Technologies, Inc., 1997.
[26] Marchessault RH. Pure Appl Chem 1962;5:107–29.
[27] Liang CY, Basset KH, McGinnes EA, Marchessault RH. Tappi 1960;43(12):1017–24.
[28] Kato K, Nitta M, Mizuno T. Agric Biol Chem 1973;37(2):433–5.
[29] Mathlouthi M, Koenig JL. Adv Carbohydr Chem Biochem 1986;44:7–89.
[30] Nelson ML, O'Connor RT. J Appl Polym Sci 1964;8:1325–41.
[31] Nelson ML, O'Connor RT. J Appl Polym Sci 1964;8:1311–24.
[32] Liang CY, Marchessault RH. J Polym Sci 1959;39:269–78.
[33] Page DH. Wood and Fiber 1976;7:246–8.